CHINESE JOURNAL OF GEOPHYSICS Vol.45, No.5, 2002, pp: 639–653

NUMERICAL STUDY ON THE EARTHWARD PROPAGATING PLASMOIDS

YANG Hong-Ang JIN Shu-Ping

(*School of Earth and Space Science, University of Science and Technology of China, Hefei* 230026, *China*)

[**Abstract**] The correlation between plasmoids and geomagnetic substorms has been demonstrated by satellite observations. In addition to the tailward propagating plasmoids with N-S bipolar signatures, earthward propagating plasmoids are found, which are characterized by plasma sheet S-N bipolar events and lobe S-N bipolar signatures. The occurrence rate of the S-N bipolar events is much lower than that of the N-S events. The S-N bipolar events occur primarily during quiet geomagnetic and IMF B_z north period, and they are correlated with small, isolated geomagnetic substorms. A 2.5 dimensional MHD simulation on the earthward propagating plasmoids has been carried out, on base of the specific distribution of the cross-tail electric fields E_y during geomagnetically quiet times (IMF B_z is northward and $\mid B_y \mid \geq B_z$). The simulation results of the two cases showed the major features of the flux rope magnetic structures and plasmoids with complex closed magnetic field lines. The similar signatures to tailward propagating plasmoids could be consistent with IMP 8 observations about the earthward propagating plasma sheet S-N bipolar events. The results displayed a similar configuration to the schema given by Schindler which may explain the low occurrence frequency of the S-N events, and also showed that the dynamic growth of the magnetic reconnection becomes considerably suppressed for a strong cross-tail magnetic field B_y. From this simulation it could be concluded that the magnetic reconnection can be the genetic mechanism of the plasma acceleration and heating in the magnetotail in both geomagnetically active and quiet time, namely, under both southward and northward (with $\mid B_y \mid \geq B_z$) IMF conditions.

[**Key words**] Plasma sheet S-N bipolar events, Geomagnetically quiet time, Cross-tail magnetic field B_y component.

1 INTRODUCTION

Plasmoids have been found to be highly correlated with geomagnetic substorm activity[1−3]. Most plasmoids are consistent with tailward propagating North-South (+/−) bipolar events[4]. In coincidence with the inflection point of the most large N-S bipolar signatures in the B_z component the B_y component shows a peak value, which are associated tailward propagating structures with flux rope cores[2,4]. Besides, plasmoid-like structures with both bipolar signatures in B_y and B_z components which resemble a "closed loop" are also identified in the analysis[5,6] of satellite data.

In addition to the tailward propagating plasmoids, the earthward propagating plasmoids with B_z South-North (S-N) bipolar signatures have also been observed with ISEE 3 in the mid-tail[5,7]. Elphic et al.[8] and Kivelson et al.[9] reported earthward propagating plasmoids with S-N bipolar signatures observed by ISEE 1/2 and Galileo, respectively.

Moldwin and Hughes[10] made a complete survey of IMP 8 magnetometer data, and identified two earthward propagating plasma sheet bipolar events, which are both characterized by B_z S-N bipolar signatures. In event 1, the B_y component shows a large magnetic core field at the inflection point of B_z. While in event 2, bipolar signatures in both B_z and B_y are the features of magnetic structures with complex closed magnetic field lines. They are very similar to two types of magnetic structures moving tailward, respectively. They also found 19 S-N bipolar lobe signatures (S-N TCRs), which have the similar characteristics to tailward propagating Traveling Compression Regions (TCRs). TCRs are indirect observational evidence for a plasmoid passage in the distant tail inferred from magnetic field signatures observed in the lobes. When a plasmoid passes downtail in the center region of the magnetotail, the magnetic flux in the tail lobes is temporarily compressed as the cross-sectional area of the lobe is reduced. This results in a transient increase in the lobe field strength and a deflection of the magnetic field vector. Such a signature has been called TCR. The statistical survey on the satellite data found that, the occurrence frequency of the earthward propagating S-N bipolar events is significantly smaller than that of the tailward propagating N-S events. They proposed that, the apparent rarity of the S-N events might be related with that they are physically small and that the S-N TCRs have shorter durations. Besides, the S-N events occur primarily under IMF B_z north and quiet geomagnetic (i.e., low-AE and -$K_{\rm p}$) conditions, when the magnetotail is in a low energy and quasi-stable state, and they are correlated with small, isolated geomagnetic substorms.

Nishida et al.[11] analyzed Geotail observations and found that during geomagnetically quiet time (when IMF B_z is northward and $\mid B_y \mid \geq B_z$) the northward magnetic field lines are convected tailward in the distant tail and they are convected earthward in the near-Earth magnetotail. Nishida et al. plotted averages of E_y against x for 11 sets of 24-hour intervals of magnetic quiescence. They found that there is a distinct change in the 24-hour average of E_y between 50 and $80R_E$: earthward of this distance E_y is clearly positive (from dawn to dusk), while beyond this distance E_y is very small and often negative (from dusk to dawn). They proposed that the reconnection can be the generic mechanism of the plasma acceleration and heating in the magnetotail in both geomagnetically active and quiet time, namely, under both southward and northward (with $\mid B_y \mid \geq B_z$) IMF conditions.

In order to study the magnetotail dynamics associated with magnetospheric substorm, many attempts have been done. Three-dimensional (3-D) simulation studies on magnetic reconnection have been worked out by Hesse and Birn[12] using a MHD code for a magnetotail model with various cross-tail magnetic field components B_y to determine the influence of B_y values on the fast dynamic evolution of the magnetotail. Their results suggested that the three-dimensional resistive tearing mode in the magnetotail works best for absent or low net cross-tail magnetic fields B_y.The dynamic growth becomes considerably suppressed for a cross-tail field of about 25% of the lobe field strength. Zhang Hong et al.[13] studied the magnetic reconnection at the magnetopause when IMF B_z is northward. They pointed out that the solar wind flow round the magnetopause lead to the formation of a shearing flow region at the nightside magnetopause, and the northward magnetic field lines of the IMF will form a shearing region of magnetic field at the shearing flow region. The magnetic reconnection occurring in this region may result in the variation of the magnetic field

topography.

A numerical study on the formation and evolution of multiple-plasmoids in the course of strong substorms with southward IMF B_z has been carried out by Jin Shuping et al.[14,15]. As well known, the magnetic cross-tail component B_y in the magnetotail is well correlated with the Interplanetary Magnetic Field (IMF) B_y component[16,17]. Based on magnetic field measurements over a large fraction of the magnetotail, Fairfield[16] found that the B_y component of IMF penetrates partially ($\approx$13%) into the magnetotail. Jin et al.[15] take two types of equilibrium solutions of the quiet magnetotail as the initial conditions of the simulation study. The numerical results of two types of cases show various features of the B_y component at the N-S (+/−) bipolar signatures of B_z component. They correspond to two kinds of tailward propagating plasmoid-like magnetic structures: one is associated with a flux rope core and the other resembles a "closed loop" plasmoid. The main characteristics of the P_3 and P_2 plasmoid events observed by Geotail on January 15, 1994 in the deep tail (x=96$R_{\rm E}$) are reproduced in the MHD simulation by Jin et al.

On basis of the above simulation studies, taking Geotail observations[11] into account, we make a simulation study on the formation and evolution of the earthward propagating plasmoids for northward (with $\mid B_y \mid \geq B_z$) IMF conditions. The simulation results display the similar features to two types of plasmoids moving tailward that are coincident with IMP-8 observations on two neutral sheet S-N bipolar events (Moldwin et al.[10]). And in some degree the low occurrence frequency of the earthward propagating S-N bipolar events can be explained by these results.

2 SIMULATION RESULTS

In this paper, we present theoretical results on the basis of an equilibrium solution of the quiet magnetotail using a MHD code with two dimensions and three components (see reference [14] for more details) to simulate the plasmoids propagating earthward. We assume that the x coordinate of a right-handed Cartesian coordinate system is in the anti-earth direction, the z coordinate is perpendicular (northward) to the plasma sheet, and the y coordinate (in dusk-dawn direction) is consistent with a right-handed coordinate system of x and z . A magnetic flux function $A(t, x, z)$ related to magnetic field is introduced by the equation:

$$\boldsymbol{B} = \nabla \times (A\boldsymbol{e}_y) + B_y \boldsymbol{e}_y \,. \tag{1}$$

We assume that the magnetotail is initially in a static equilibrium state and $A(x, z)$ is weak variations with respect to x. A class of tail-like equilibrium solution is given by the following expression:

$$A(x, z) = B_\infty L_{\rm c}[\ln\cosh(\frac{H(x)z}{L_{\rm c}}) - \ln H(x)] \,, \tag{2}$$

where B_∞ is the initial value of B_x at $t = 0$ and $z = L_z$, and $H(x)$ varies slightly in x and is expressed by

$$H(x) = (1.0 + \frac{bx}{\nu L_{\rm c}})^{-\nu} \,, \tag{3}$$

in this report, we set $b = 0.018$, $\nu = 0.6$, $L_{\rm c} = 2R_{\rm E}$.

For the case with uniform initial temperature T_0, using Eq.(2), two types of the plasma density $\rho(x,z)$ and magnetic $B_y(x,z)$ component can be obtained as follows:

Type I:

$$B_y = 2\mathrm{nT} \tag{4}$$

$$\rho(x,z) = \rho_\infty + \rho_\mathrm{c}\left[\frac{H(x)}{\cosh(\frac{H(x)z}{L_\mathrm{c}})}\right]^2 \tag{5}$$

where ρ_∞ is the initial plasma density on the boundary of the magnetic tail ($z = L_z$). The density at $\rho(0,0) = \rho_\infty + \rho_\mathrm{c}$ at $x = 0$ and $z = 0$. Here $\rho_\mathrm{c} = B_\infty^2/8\pi RT_0$ (R is the gas constant).

Type II:

$$B_y(x,z) = \sqrt{1-\alpha}B_\infty\frac{H(x)}{\cosh(\frac{H(x)z}{L_\mathrm{c}})}, \tag{6}$$

$$\rho(x,z) = \rho_\infty + \alpha\rho_\mathrm{c}\left[\frac{H(x)}{\cosh(\frac{H(x)z}{L_\mathrm{c}})}\right]^2, \tag{7}$$

where α is a constant with values $0 < \alpha \leq 1$. It can be found by comparing (4), (5) with (6), (7), that the distribution of B_y in Type I is significantly different from that in Type II, but the distribution of plasma density in Type I is similar to that in Type II. It can also be seen from (6) and (7) that $\rho(x,z)$ increases and $B_y(x,z)$ decreases with α increasing and $B_y = 0$ when $\alpha = 1.0$. In the present study, we take $T_0 = 1.66\times10^6$K, $\rho_\infty = 1.67\times10^{-25}\,\mathrm{g/cm^3}$ (corresponding to the density of *ion* n_i=0.1/cm^3), $B_\infty = 17.3\,\mathrm{nT}$, and $\rho_\mathrm{c} = 4.34\times10^{-24}\,\mathrm{g/cm^3}$ (corresponding to n_i=2.6/cm^3), $B_\mathrm{c} = 10\,\mathrm{nT}$. Hence the Alfven velocity is $v_A = B_\mathrm{c}/\sqrt{4\pi\rho_\infty}$=690.3 km/s, and the characteristic time is given by $\tau_\mathrm{A} = L_z/v_\mathrm{A}$=184.6 s.

The simulation system is assumed to be initially in a static isothermal state, that is $v_x = v_y = v_z = 0$ and $T = T_0$. Two types of equilibrium solutions of a quiet magnetotail are used as the initial state of the simulation study. The lengths of the simulation box in the z direction and the x direction are taken to be $L_z = 20R_\mathrm{E}$, $L_x = 110R_\mathrm{E}$ (the unit of length is set as $l_0 = L_z$). Since symmetric boundary conditions are imposed at the bottom boundary ($z = 0$), the simulation is carried out in the upper half plane of the magnetotail. The computational domain $0 \leq x \leq L_x$, $0 \leq z \leq L_z$ is divided into 56×23 mesh points. In order to allow adequate special resolution in the neutral sheet, the grid spacing in the z direction increases according to a geometric series and a uniformed mesh is adopted along the x direction.

Assuming a dawn-dusk electric field $\boldsymbol{E}$ is imposed on the boundary of the magnetotail, plasma inflow are generated by both $\boldsymbol{E}$ and magnetic field $\boldsymbol{B}$ along the top boundary ($z = L_z$): $v_z = -\dfrac{cEB_x}{B^2}$, $v_x = \dfrac{cEB_z}{B^2}$.

On the basis of the Geotail observations[11], during geomagnetically quiet time (IMF B_z is northward and $|\,B_y\,| \geq B_z$) earthward of the distance ($x \approx 50R_\mathrm{E}-80R_\mathrm{E}$) E_y is directed from dawn to dusk. We take $L_x = 110R_\mathrm{E}$. We assume that along the top boundary ($z = L_z$), the electric field E is uniform in the range of $0 \leq x \leq 50R_\mathrm{E}$ and $\boldsymbol{E}$ decreases linearly to zero in the range of $50R_\mathrm{E} < x \leq 60R_\mathrm{E}$, and $\boldsymbol{E}$ remains zero within $60R_\mathrm{E} < x \leq 110R_\mathrm{E}$ where

$\boldsymbol{E}$ is a dimensionless electric field imposed on the boundary in units of $E^* = v_{\rm A}B_\infty/c$ (c is the velocity of light). For the cross-tail width $L_y = 40R_{\rm E}$, the cross-tail potential drop corresponds to $E_0 = 0.1$ to about 300 kV. In this paper, we take $E_0 = 0.12$. The plasma inflow generated by the magnetic field and dawn-dusk electric field are imposed on the top boundary of the magnetotail within the range of $x \leq 60R_{\rm E}$.

2.1 Case 1

The magnetic flux function $A(x, z)$, magnetic field $B_y(x, z)$ component, and the plasma density $\rho(x, z)$ at the time of $t = 0$ are expressed by (2), (4), (5), that is Type I. Under the action of the plasma inflow imposed on the boundary, magnetic reconnection occurs in the neutral sheet of the magnetotail. And the simulation results are shown in Fig. 1.

The time evolution of the magnetic field configuration is plotted in Fig. 1(a), which shows the formation and evolution of six small magnetic structures. The first panel ($t = 0$) shows the equilibrium state of the magnetotail. It can be seen in the panel at $t = 27.2\tau_{\rm A}$ that the plasma sheet thinning occurs at about $x \approx 25R_{\rm E}$ and an X-type neutral point forms there. Earthward and tailward of the neutral point, the magnetic field lines departed from the initial configurations. A small bubble-like magnetic structure forms at $x \approx 20R_{\rm E}$, and at $t = 32.4\tau_{\rm A}$ the structure moves earthward and its size grows a little. But the reconnection does not develop further, and ceases before reaching the magnetic field lines far from the neutral sheet. At $t = 33.5\tau_{\rm A}$, the small structure is trapped within the field lines near the Earth and combined with them. The second structure, appearing earthward of the reconnection site at $t = 45.7\tau_{\rm A}$, is soon trapped before developing further, and it combined with the closed field lines at $t = 47.4\tau_{\rm A}$. The developments of the small structures during the periods $69.4 - 72.8\tau_{\rm A}$, $86.7 - 87.9\tau_{\rm A}$, $137.0 - 138.7\tau_{\rm A}$, and $164.7 - 168.2\tau_{\rm A}$ are almost the same as those just described. What is common in them is as follows, the magnetic reconnection occurs in the neutral sheet of the magnetotail, and at about $x{\approx}25 - 30R_{\rm E}$ an X-type neutral point forms, at the Earth-side of the neutral point a small bubble-like magnetic structure appears. But the reconnection ceases before reaching the lobes, and small magnetic structures are soon trapped within closed field lines and combine with them.

The time variations of the total magnetic field amplitude $B(= \sqrt{B_x^2 + B_y^2 + B_z^2})$ and the three components B_x, B_z, B_y at a given point ($x = 14R_{\rm E}$, $z = -0.3R_{\rm E}$) in the neutral sheet are shown in Fig. 1(b). As shown in the B_z curve, at $t{\approx}45.7\tau_{\rm A}$, $67.1\tau_{\rm A}$, $72.6\tau_{\rm A}$, $87.9\tau_{\rm A}$, $137.9\tau_{\rm A}$, and $169.6\tau_{\rm A}$ when a plasmoid passes through this point the obvious $-/+$ bipolar signature in the B_z component, which is similar to the observational feature of the current sheet S-N bipolar events, can be found. It is notable that in coincidence with the inflection point of the B_z bipolar signatures, the B_y component shows a peak value. It means that, for case 1 with the initial uniform distribution of B_y component (Type I), the B_y component within the small magnetic structures formed near the Earth shows a peak value. This is an important feature of a flux rope structure, which is similar to the feature of the current sheet S-N bipolar event 1 observed by IMP-8 (Moldwin and Hughes[10]). But the southward amplitude of the S-N bipolar signatures in Fig. 1(b) is very small and the bipolar characteristics are not so typical. This may be related to the small scales of the bubble-like magnetic structures, which only cause the southward deflection of the magnetic field lines while passing through the neutral sheet near the Earth. For the same reason,

the small magnetic structures only cause a little change of B_x component passing through the point of $x = 14R_{\rm E}$, $z = -0.3R_{\rm E}$ near the Earth which is shown by the small variation amplitude in the $B_x - t$ curve in Fig. 1(b). As shown in the $B - t$ curve, at the inflection point of the B_z bipolar signatures the total magnetic field B shows a little peak value, which corresponds to the peak value of B_y component, namely, the enhancement of total magnetic field B results from the B_y maximum.

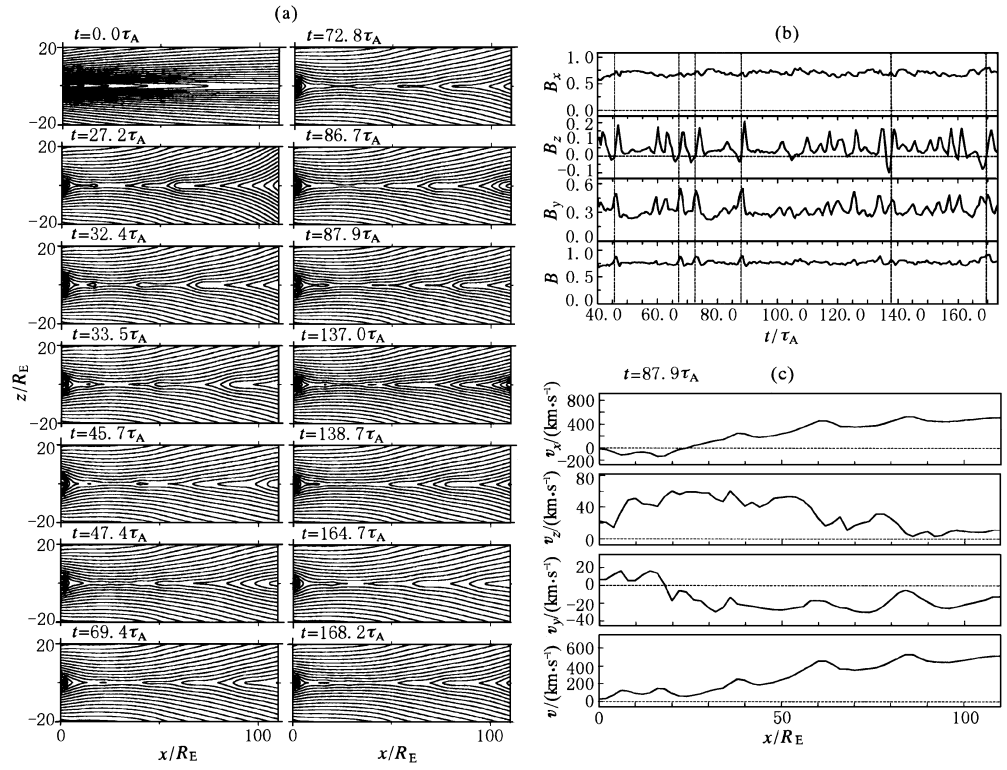

Fig. 1 Simulation results for case 1

(a) The time evolution of the magnetic field configuration in case 1; (b) The time variations of the total magnetic field amplitude B and the three components B_x, B_z, B_y at a given point ($x = 14R_{\rm E}$, $z = -0.3R_{\rm E}$) in the neutral sheet in case 1; (c) The distributions of the velocity v and the v_x, v_y, v_z components along x in the current sheet ($z = -0.3R_{\rm E}$) at $t = 87.9\tau_{\rm A}$ in case 1.

The distributions of the velocity $v(= \sqrt{v_x^2 + v_y^2 + v_z^2})$ and the v_x, v_y, v_z components along x in the current sheet ($z = -0.3R_{\rm E}$) at $t = 87.9\tau_{\rm A}$ is shown in Fig. 1(c). It can be seen from the figure that the direction of v_x reversed at about $x \approx 25R_{\rm E}$, and that is where the X-type neutral point lies. The location of X neutral point also can be seen from the configuration of magnetic field line at the same time in Fig. 1(a). Earthward of the reconnection point, v_x<0, the plasma moves toward the Earth and the maximum flow speed is –180 km/s, while at the tail-side the plasma moves toward the far tail ($v_x > 0$) with the maximum speed of about 550 km/s. It can be seen in the $v_x - x$ curve that the tailward moving velocity is about 270 km/s at $40R_E$, 410 km/s at $70R_{\rm E}$, and it reaches 520 km/s at $100R_{\rm E}$, which indicates the acceleration of plasma motion, which is approximately consistent

with observations. We can also see from the $v_z - x$ and $v_y - x$ curves that the maximum of v_z is about 60 km/s, and $|v_y|<30\,km/s$, so the v_z and v_y are far less than v_x. Hence, the plasma velocity in the neutral sheet of the magnetotail is mainly decided by v_x and a high-speed tailward moving flow exists at $x>50R_{\rm E}$. As seen in the $v - x$ curve, the velocity v increases from minimum 70 km/s at the reconnection point to 600 km/s at the right boundary. That means the magnetic energy is transformed into kinetic energy in the course of reconnection.

2.2 Case 2

The magnetic flux function $A(x, z)$, magnetic field $B_y(x, z)$ component, and the plasma density $\rho(x, z)$ at time $t = 0$ are expressed by (2), (6), (7), respectively, that is Type II. And we take $\alpha = 0.7$, the simulation results are shown in Fig. 2.

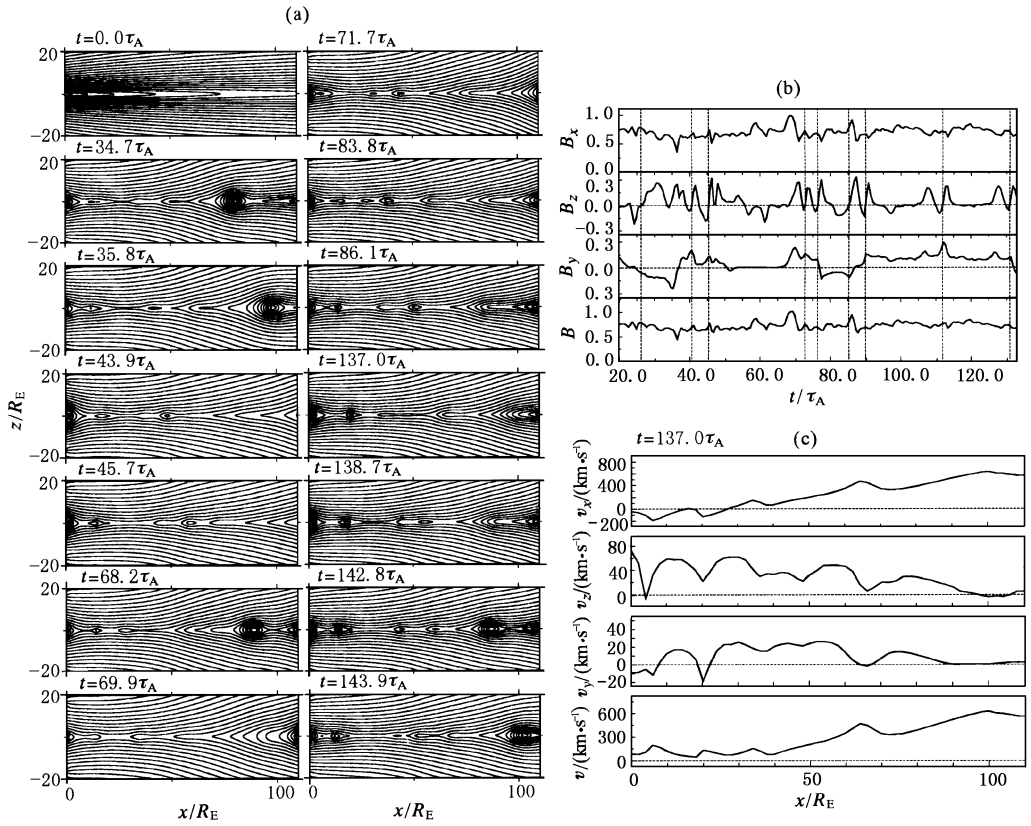

Fig. 2 Simulation results for case 2

(a) The time evolution of the magnetic field configuration in case 2; (b) The time variations of the total magnetic field amplitude B and the three components B_x, B_z, B_y at a given point ($x = 14R_{\rm E}$, $z = -0.3R_{\rm E}$) in the neutral sheet in case 2; (c) The distributions of the velocity v and the v_x, v_y, v_z components along x in the current sheet ($z = -0.3R_{\rm E}$) at $t = 137.0\tau_{\rm A}$ in case 2.

The time evolution of the magnetic field configuration is shown in Fig. 2(a), which displays the formation and evolution process of five small magnetic structures. An X-type neutral point forms at the distance of $x \approx 28R_{\rm E}$ at $t \approx 34.7\tau_{\rm A}$ and a small magnetic structure appears earthward of the neutral point. It is trapped within the closed field lines

near the Earth before developing further, and is soon combined with them under the action of the earthward moving flows (see the panel at $t = 35.8\tau_{\rm A}$). A plasmoid forms at the tail-side of the reconnection point, and its size grows obviously while it moves tailward. At $t = 38.5\tau_{\rm A}$ it reaches the right boundary and departs from the simulation box. The plasmoid events occurring during intervals of $43.9 - 45.7\tau_{\rm A}$, $68.2 - 71.7\tau_{\rm A}$, $83.8 - 86.1\tau_{\rm A}$, and $137.0 - 143.9\tau_{\rm A}$ are almost the same as those just described. What is common in them is as follows, the magnetic reconnection occurs in the neutral sheet of the magnetotail, and an X-type neutral point forms at about $x{\approx}25 - 30R_{\rm E}$; At the Earth-side of the reconnection point small plasmoid-like magnetic structures form, and they are soon trapped within closed field lines and combine with them because the reconnection ceases before reaching the lobes; At the same time, plasmoids form at the tail-side of the reconnection point and they grow gradually in tailward propagation.

Fig. 2(b) displays the time variations of the total magnetic field strength B and the three components B_x, B_z, B_y. It can be seen from the $B_z - t$ curve, that the B_z component displays $-/+$ (S-N) bipolar signatures, indicating the passage of a plasmoid through the observation site. But in coincidence with the inflection point of the B_z bipolar signatures, the B_y component displays a complex pattern, which is quite different from Fig. 1(b). At some inflection points of B_z component, e.g., $t{\approx}25\tau_A$, $76\tau_A$, $86\tau_{\rm A}$, and $131\tau_{\rm A}$, the B_y component also shows a bipolar signatures, suggesting a small magnetic structure with complex closed field lines, and they have features similar to the current sheet S-N bipolar event 2 observed by IMP 8 (Moldwin and Hughes[10]). But another case also exists, the B_y has a rather large value when a plasmoid passes, e.g., at $40.6\tau_A$, $45.4\tau_{\rm A}$, $72.8\tau_{\rm A}$, $89.9\tau_{\rm A}$, and $111.9\tau_A$. The $B_x - t$ curve in Fig. 2(b) shows a wavelike variation with the variation amplitude greater than that in Fig. 1(b). This may be related with that there are plasmoids with large scales at the tail-side of the reconnection point in case 2. In Fig. 2(b) the $B - t$ curve varies just like the $B_x - t$ curve, because the variation amplitude of $B_x - t$ is rather greater than that of the $B_y - t$ curve and the B_x plays a dominant role in the time evolution of magnetic field amplitude B.

The distributions of velocity v and the three components v_x, v_y, v_z in the current sheet ($z = -0.3R_{\rm E}$) along x at time $t = 137.0\tau_A$ are given in Fig. 2(c). It can be seen from the figure that the direction of v_x reversed at about $x{\approx}26R_{\rm E}$, and that is where the X-type neutral point forms. The location of X neutral point also can be found from the magnetic field configuration at the same time in Fig. 1(a). Earthward of the reconnection point $v_x{<}0$, the plasma moves toward the Earth and the maximum speed is –180 km/s, while at the tail-side the plasma moves toward the far tail ($v_x > 0$) with the maximum speed of about 600 km/s. The tailward moving velocity v_x increases with increasing x which indicates the similar acceleration motion of the plasma to case 1. It can be found from the $v_z - x$ and $v_y - x$ curves that v_z is less than 70 km/s and $\mid v_y \mid{<}30$ km/s, and thus the v_z and v_y are far less than v_x. The plasma velocity flow is mainly decided by v_x, namely, there is tailward plasma. The velocity v increases from the minimum value (70 km/s) at the reconnection point to 600 km/s at the right boundary which indicates that the magnetic energy is transformed into kinetic energy in the course of reconnection.

As mentioned above, case 1 and case 2 are the numerical simulations on the magnetotail

reconnection in geomagnetically quiet time (IMF B_z is northward and $|B_y| \geq B_z$), and the numerical results are in line with the features of the two neutral sheet S-N bipolar events observed by IMP 8. The observations[2,10,18] show that most plasmoids have strong core field and are a kind of magnetic structures with flux rope core which has been reproduced in case I. Reference [15] investigated the magnetotail reconnection in geomagnetically active time (IMF B_z is southward). In the simulation, Jin et al. assumes that the south-directing field lines are convected tailward and the dawn-dusk electric field $\boldsymbol{E}$ are imposed on the boundary of the magnetotail in a large range. Case I-(1) ($E_0 = 0.08$) and case I-(2) ($E_0 = 0.05$) with the initial state of Type I in reference [15] display the tailward propagating process of the magnetic structures with flux rope core. In order to investigate the influence of the range imposed by the dawn-dusk electric field $\boldsymbol{E}$, case 3 is introduced.

2.3 Case 3

At the time of $t = 0$, $A(x, z)$, $B_y(x, z)$ and $\rho(x, z)$ are expressed by (2), (4), (5) respectively, and the initial state is set as Type I. Along the top boundary ($z = L_z$) the electric field $\boldsymbol{E}$ is uniform in the range of $0 \leq x \leq 100R_{\rm E}$ and $\boldsymbol{E}$ decreases linearly to zero in the range of $100R_{\rm E} < x \leq 110R_{\rm E}$. Under the action of plasma inflow caused by the simultaneous effect of the electric field $\boldsymbol{E}$ and magnetic field $\boldsymbol{B}$, the magnetotail reconnection occ

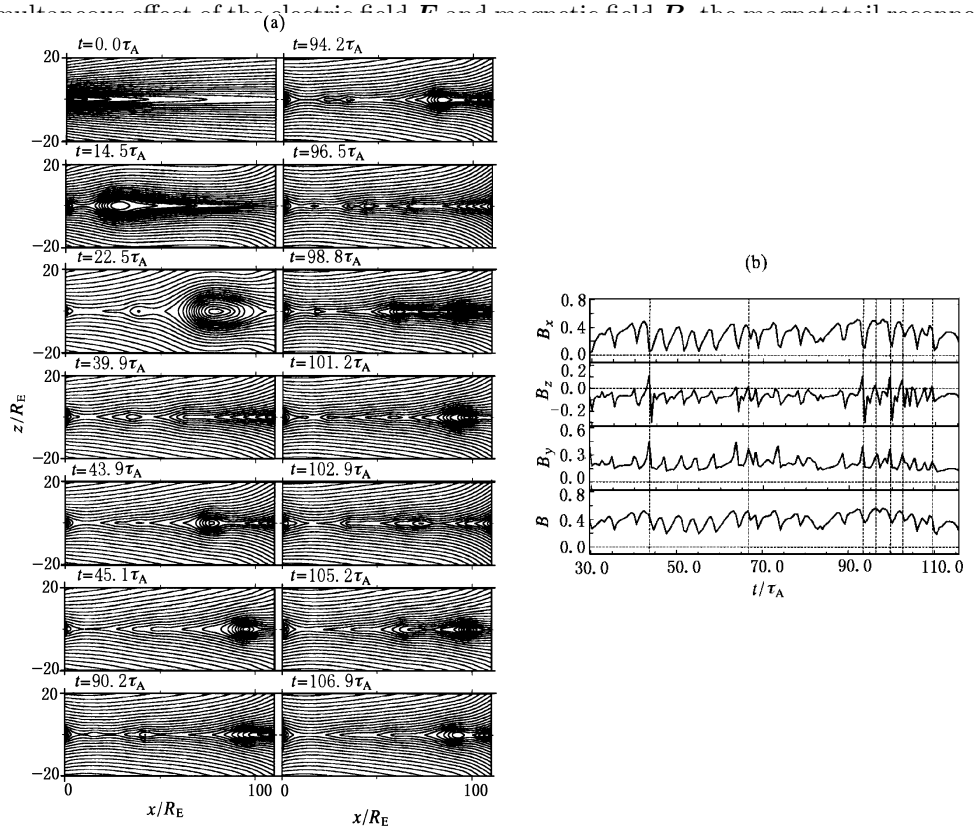

Fig. 3 Simulation results for case 3

(a) The time evolution of the magnetic field configuration in case 3; (b) The time variations of the total magnetic field amplitude B and the three components B_x, B_z, B_y at a given point ($x = 70R_E$, $z = -0.3R_E$) in the neutral sheet in case 3.

Fig. 3(a) shows the time evolution of magnetic field configuration. As seen in Fig. 3(a) the multiple X-line reconnection occurs intermittently under the action of the plasma inflow. The X-type neutral point forms at $x \approx 20 - 25R_{\rm E}$. At the Earth-side of the reconnection point there are small magnetic structures and they are soon trapped within closed field lines and combine with them. It is obviously different from case 1 that the plasmoids form repeatedly at the tail-side of the reconnection point and grow gradually in the propagation toward down tail. This feature displayed that multiple plasmoids are formed repeatedly and ejected tailward in the course of strong substorms during geomagnetically active time.

The time variations of the total magnetic amplitude B and the three components B_x, B_z, B_y are displayed in Fig. 3(b). As seen in the $B_z - t$ curve, at times of $43.5\tau_{\rm A}$, $66.6\tau_{\rm A}$, $93.2\tau_{\rm A}$, $96.2\tau_{\rm A}$, $99.6\tau_{\rm A}$, $102.5\tau_{\rm A}$, and $109.3\tau_{\rm A}$, the B_z component shows a $+/-$ (N-S) bipolar signatures, indicating the passage of a tailward moving plasmoid through the given point. In coincidence with the inflection point of the B_z N-S bipolar signatures, the B_y component shows a peak value, whereas the B_x component shows a depressed value and the field magnitude B is between a peak and a minimum value. The center of a plasmoid corresponds to a largest B_y value, which represents an important feature for a plasmoid-like structure with flux rope core. In the $B_x - t$ and $B - t$ curves in Fig. 3(b), $B_x < 0.5$, $B < 0.6$, and they are obviously smaller than those values in Fig. 1(b). Such a difference is related to the different observation sites taken in the two cases. The observation sites in Fig. 3(b) and 1(b) are chosen to be at ($x = 70R_{\rm E}$, $z = -0.3R_{\rm E}$) and ($x = 14R_{\rm E}$, $z = -0.3R_{\rm E}$), respectively. In the expression (1) $B_x = -\frac{\partial A}{\partial z}$ and $|B_x|$ decreases with increasing x, which can be easily seen from the expressions (2) and (3).

3 DISCUSSIONS AND CONCLUSIONS

3.1 The initial conditions of both case 1 and case 3 are set as Type I and the uniform electric field $\boldsymbol{E}$ of two cases are taken as 0.12. The difference between case 1 and case 3 is that the electric fields $\boldsymbol{E}$ are imposed on different ranges. Both of them correspond to geomagnetically quiet (IMF B_z is northward and $\mid B_y \mid \geq B_z$) and active (IMF B_z is southward) time. The results indicate that in case 1 (Fig. 1(a)) only small magnetic structures move earthward, while there are plasmoids with large scales ejected toward down tail in case 3 (Fig. 3(a)). The S-N $(-/+)$ and N-S $(+/-)$ bipolar signatures of the B_z components are displayed in Fig. 1(b) and Fig. 3(b), respectively. In coincidence with the inflection points of the B_z bipolar signatures the B_y component shows a peak value in both cases, which represent the basic features of flux rope structures moving earthward and tailward. The observations indicate that most plasmoids are consistent with magnetic flux ropes. In case 1 the initial B_y value in the magnetotail is taken as 2 nT, and the corresponding IMF B_y is greater than $10nT$ (B_y (magnetotail)$\approx 0.13 B_y$(IMF)), which is coincidence with the condition IMF $\mid B_y \mid \geq B_z$. Hence the simulation results suggest that the reconnection can be the generic mechanism of the plasma acceleration and heating in the magnetotail in both geomagnetically active and quiet time, namely, under both southward and northward (with $\mid B_y \mid \geq B_z$) IMF conditions.

3.2 Fig. 4, adapted from Schindler[19], demonstrates the magnetic configuration in the magnetotail reconnection with two magnetic structures labeled "A" and "B". At earthward

side of the X-type neutral point magnetic reconnection ceases before reaching the tail lobes and the magnetic structure labeled "A" is trapped within closed field lines, while at tailward side of the reconnection point, magnetic reconnection continues to the lobes and the magnetic structure labeled "B" with a large scale disconnects from the Earth. The simulation results reproduce this schema. Case 1 and case 2 with different initial conditions are the numerical experiments during geomagnetically quiet time (IMF B_z is northward and $\mid B_y \mid \geq B_z$). As is seen from Fig. 1(a), a small bubble-like magnetic struc-ture forms at the Earth side of the reconnection point and soon it is trapped within closed field lines and combine with them. As shown in Fig. 1(a) the small magnetic bubbles are quite similar to the magnetic structure labeled "A" in the schema. The major difference between Fig. 1(a) and the schema is that there is no a plasmoid formed at tailward side of the reconnection point. The time evolution of magnetic field configuration of case 2 is shown in Fig. 2(a). The small magnetic structures formed at the earth-side of the reconnection point are trapped by the closed field lines, just as in case 1. At the tail-side of the reconnection point plasmoids are generated. As shown in Fig. 2(a), the plasmoids depart from the Earth and grow in tailward propagation, which is more similar to the schema (Fig. 4) given by Schindler[19].

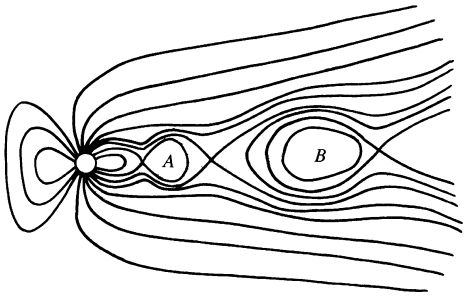

Fig. 4 A schematic of the noon-midnight meridional cross-section of the nightside magnetosphere[19]

As is shown in Figs. 1(a) and 2(a), the magnetic structures with small scales formed earthward of the reconnection point are trapped within closed field lines and combined with them, rapidly. So, those earthward moving structures have short durations. It can be found from Fig. 1(b) and Fig. 2(b) that the B_z component displays a S-N (−/+) bipolar signatures when the small magnetic structures pass through the magnetotail neutral sheet in the near Earth region. The south amplitude of the bipolar signatures is too small, and the bipolar feature is not so obvious that could result in the low occurrence frequency of the earthward propagating current sheet S-N bipolar events. What's more, in order to analyze the lobe S-N bipolar signatures (S-N TCRs), we also plot time variations of magnetic amplitude B and the three components B_x, B_z, B_y at a point in the lobes near the Earth. We make plots at $x = 14R_E$ with various z value and find that the reduction of the cross-sectional area of the lobe is very slight and the transient increase in the lobe strength and the deflection of the magnetic field vector resulted from the compression of the magnetic flux in the tail lobes are not obvious at $|z|>3R_E$ in case 1 and at $|z|>4R_E$ in case 2 when a very small plasmoid passes through the current sheet of the magnetotail. These may interpret the low detective frequency of the S-N TCRs.

It should be pointed out that the X-type neutral points in case 1 and case 2 lie at about $25-30R_E$, and they are too near to the near-Earth boundary, and this may be related with the too small sizes of the earthward propagating plasmoids. According to the observations analyzed by Nishida et al.[11], we assume dawn-dusk electric field $\boldsymbol{E}$ to be uniform along

the boundary of the magnetotail in range of $0 \leq x \leq 50 R_{\rm E}$. We have made simulations with various $\boldsymbol{E}$ value, but we still couldn't find a case with reconnection points far from the left boundary ($x \geq 50 R_{\rm E}$).

3.3 Observations indicate that the earthward propagating magnetic structures have features similar to the tailward propagating plasmoids. In this paper, we take equilibrium solutions of Type I and Type II as the initial states of case 1 and case 2, respectively. The numerical results indicate that the S-N $(-/+)$ bipolar signatures of B_z component are accompanied with different features of the B_y component. They are consistent with the earthward propagating flux rope structures and magnetic structures with complex closed field lines, respectively, and they are in line with the two current sheet S-N bipolar events detected by IMP 8 (Moldwin et al.[10]). We propose that the different topography of the earthward propagating magnetic structures may be correlated with the different distributions of magnetotail B_y component. Similar conclusions were also drawn in the simulation study on the tailward propagating multiple plasmoids. The formation and evolution of magnetic helicity of various magnetic structures in the magnetotail has been analyzed by CUI Hai-Long et al[20]. It is unnecessary to go into details in this paper.

Both case 1 and case 2 are aimed at the geomagnetically quiet time (IMF B_z is northward and $\mid B_y \mid \geq B_z$), and there is a difference only in the initial conditions between case 1 and case 2. Comparing Fig. 1(a) and Fig. 2(a), we find great differences in the magnetic reconnection evolutions between Fig. 1(a) and Fig. 2(a). Small magnetic structures in Fig. 1(a) form only earthward of the reconnection site, while tailward of it there is almost no obvious plasmoids. But in Fig. 2(a) magnetic structures formed eathward of the reconnection site have larger sizes than those in Fig. 1(a), and there are also plasmoids formed at tailward side of the reconnection point. It is obvious that the reconnection process of case 2 is faster than that of case 1. To understand the intermittent features, we study the time variations of the reconnection flux function. The definition of the reconnection flux function is determined by the following expression: $\Phi = (\triangle A)_t - (\triangle A)_0$, where $(\triangle A)_t$ and $(\triangle A)_0$ are the differences between the maximum and the minimum of the normalized magnetic flux function A at time t and time $t = 0$, respectively. We can see from Fig. 5(a) that the $\Phi - t$ curve displays a waveform variation, which is associated with that in case 1 only small magnetic structures are formed earthward of the reconnection site and are trapped before the magnetic reconnection develops further. However, there are some obvious peak values in Fig. 6(a). In comparison with Fig. 2(a) we find that the peak value at time $43.9 - 45.7\tau_{\rm A}$ in Fig. 6(a) corresponds to a large plasmoid tailward of the reconnection point in Fig. 2(a), and the peak values at times $45 - 50\tau_{\rm A}$ and $60 - 70\tau_{\rm A}$ in Fig. 6(a) are associated with the formation and evolution of small magnetic structure at $43.9 - 45.7\tau_{\rm A}$ and with the development of the plasmoid tailward of the reconnection point at times $68 - 70\tau_{\rm A}$ in Fig. 2(a), respectively. There are also plasmoids formed at about $110\tau_{\rm A}$, but Fig. 2(a) is emphasized on the evolution of the magnetic structures at the Earth-side, and the process is not displayed here.

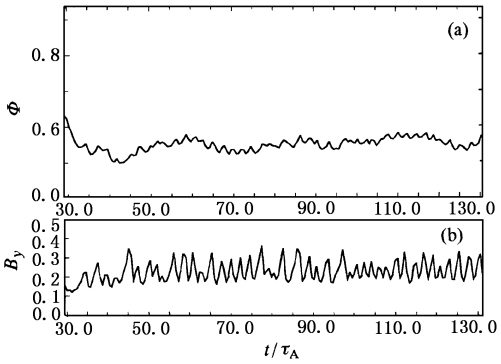

Fig. 5 The time variations of (a) the reconnection flux function Φ and (b) B_y in case 1

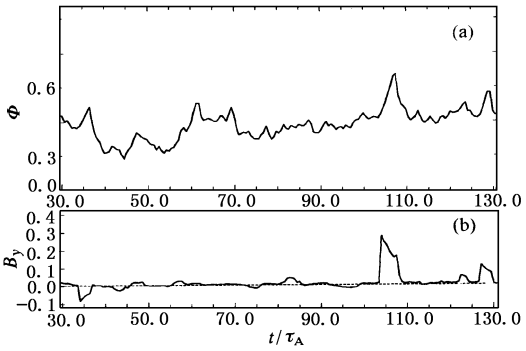

Fig. 6 The time variations of (a) the reconnection flux function Φ and (b) B_y in case 2

Then why are there such great differences in the reconnection process between the two cases? We study the time evolution of the B_y component to seek answers. In this simulation, the maximum of magnetic flux function A is at the boundary ($z = L_z$) and the minimum value lies in the current sheet, especially at the O-type neutral point. Fig. 5(b) and Fig. 6(b) give the time variations of B_y component at the point where A is the minimum in case 1 and case 2, respectively. As can be seen from Fig. 5(b), the B_y value shows a saw-like variation with its value from 0.15 to 0.35, and the average is about 0.25. The $B_y - t$ curve in Fig. 6(b) displays a waveform variation about $B_y = 0$. As shown in Fig. 6(b) only in quite short intervals $\mid B_y \mid > 0.05$ and the B_y average is obviously lower than that of case 1. Hence, the magnetic reconnection in case 2 develops faster than that in case 1 which may be related with the low B_y value in the magnetotail current sheet. The strong cross-tail B_y component has a close control over the magnetotail dynamic process which can be found from the suppressed reconnection process in case 1. Similar conclusions are also drawn by Hesse et al.[12] in their study on the influence of the B_y values on the fast dynamic evolution of the magnetotail.

From the above analysis the main conclusions are as follows:

(1) The simulations in this paper during geomagnetically quiet (IMF B_z is northward and $\mid B_y \mid \geq B_z$) and active (IMF B_z is southward) time display the basic characteristics of earthward and tailward propagating flux rope structures. And we propose that the magnetic reconnection is the generic mechanism of the plasma acceleration and heating in the magnetotail in geomagnetically either active (IMF B_z is southward) or quiet (IMF B_z is northward and $\mid B_y \mid \geq B_z$) time.

(2) The simulation results indicate that the small magnetic structures formed at earthward side of the reconnection point are trapped within closed field lines near the Earth before developing further. Such plasmoids with small sizes and short duration is the main cause of the low detective frequency of the earthward propagating S-N bipolar events. When

the small plasmoids pass through the current sheet in the magnetotail, the enhancement of the magnetic strength and the deflection of the magnetic direction in the lobes are slight which may be related to the rare occurrence of S-N TCRs.

(3) We take two types of equilibrium solutions as the initial states of case 1 and case 2, and the simulation results display the main features of two types of earthward propagating S-N bipolar events with flux rope core and with both B_y and B_z bipolar signatures. Therefore, the different topography of the earthward propagating magnetic structures may be related to the different distributions of B_y component in the magnetotail.

(4) The reconnection development of case 2 is faster than that of case 1, which is associated with the lower B_y value in the neutral sheet for case 2 than that for case 1. It can be easily found from the $\Phi - t$ curve and $B_y - t$ curve that the enhancement of cross-tail B_y component in the neutral sheet considerably suppressed the dynamic growth of the reconnection in the magnetotail.

ACKNOWLEDGMENTS

This work was supported by the National Natural Science Foundation of China (40174042, 49834040) and the Innovation Engineering Fund of the USTC.

REFERENCES

[1] Hones E W, baker Jr D N, Bame S J, et al. Structure of the magnetotail at 220 R_E and its response to geomagnetic activity. *Geophys. Res. Lett.*, 1984, **11**: 5–7.

[2] Slavin J A, Baker D N, Craven J D, et al. CDAWS observations of plasmoid signatures in the geomagnetic tail: An assessment. *J. Geophys. Res.*, 1989, **94**: 15 153–15 175.

[3] Nagai T, Takahashi K, Kawano H, et al. Initial GEOTAIL survey of magnetic substorm signatures in the magnetotail. *Geophys. Res. Lett.*, 1994, **21**: 2 991–2 994.

[4] Moldwin M B, Hughes W J. Plasmoids as magnetic flux ropes. *J. Geophys. Res.*, 1991, **96**: 14 051–14 064.

[5] Moldwin M B,Hughes W J. On the formation and evolution of plasmoids: A survey of ISEE3 Geotail data. *J. Geophys. Res.*, 1992, **97**: 19 259–19 282.

[6] Zong Q G, wilken B, Reeves G D, et al. Geotail observations of energetic ion species and magnetic field in plasmoid-like structure in the course of an isolated substorm event. *J. Geophys. Res.*, 1997, **102**(A6): 11 409–11 428.

[7] Nishida A, Scholer M, Terasawa T, et al. Quasi-stagnant plasmoid in the middle tail: A new pre-expansion phase phenomenon. *J. Geophys. Res.*, 1986, **91**: 4 245–4 255.

[8] Elphic R C, Cattell C A, Takahashi K, et al. ISEE-1 and 2 observations of magnetic flux ropes in the magnetotail: FTEs in the plasma sheet? *Geophys. Res. Lett.*, 1986, **13**: 648.

[9] Kivelson M G, Kennel C F, Mcpherron R L, et al. The Galileo Earth encounter: Magnetometer and allied measurements. *J. Geophys. Res.*, 1993, **98**: 11 299–11 318.

[10] Moldwin M B, Hughes W J. Observations of Earthward and tailward propagating flux rope plasmoids: Expanding the plasmoid model of geomagnetic substorms. *J. Geophys. Res.*, 1994, **99**: 183–198.

[11] Nishida A, Mukai T, Yamamoto T, et al. A unified model of the magnetotail convection in geomagnetically quiet and active times. *J. Geophys. Res.*, 1998, **103**: 4 409–4 418.

[12] Hesse M, Birn J, Sydora R D, et al. The coalescence of magnetic flux ropes and reconnection in the magnetotail. *J. Geophys. Res.*, 1990, **94**: 2 471–2 483.

[13] ZHANG Hong, LIU Zhen-Xing. A Global Model of magnetic reconnection at magnetopause for northward IMF. *Chinese Journal of Space Science*, 1996, **16**(4): 274–281.

[14] JIN Shu-Ping, HU Xian-Peng, CUI Hai-Long, et al. A preliminary exploration of the mechanism for the occurrence of two types of various magnetic structures in the magnetotail. *Chinese Science Bulletin*, 2001, **46**(12): 981–986.

[15] Jin S P, Hu X P, Zong Q G, et al. A 2.5 dimensional MHD simulation of multiple-like structures in the course of a substorm. *J. Geophys. Res.*, 2001, **106**(A12): 29 807–29 830.

[16] Fairfield D H. On the average configuration of the geomagnetic tail. *J. Geophys. Res.*, 1979, **84**: 1 950–1 953.

[17] Lui A T Y. Characteristics of the cross-tail current in the earth's magnetotail. In: Potemra T A, ed. Washington D C: AGU publishers. *Geophysical Monograph Ser.*, 1984, **28**: 158–170.

[18] Ieda A, Machida S, Mukai T, et al. Statistical analysis of the plasmoid evolution with Geotail observations. *J. Geophys. Res.*, 1998, **103**: 4 453–4 465.

[19] Schindler K. A theory of the substorm mechanism. *J. Geophys. Res.*, 1974, **79**: 2 803.

[20] CUI Hai-Long, JIN Shu-Ping. The evolution of magnetic helicity of various magnetic structures in the magnetotail. *Chinese J. Geophys.*, 2002, **45**(2): 149–159.